The SNARE-associated protein Sft2 functions in Imh1-mediated SNARE recycling transport upon ER stress

Chun-Chi Lai[a,b], Wan-Yun Chiu[a,b], Yan-Ting Chen[a,b], Chia-Lu Wu[a,b], and Fang-Jen S. Lee[a,b,c,*]
[a]Institute of Molecular Medicine; [b]Center of Precision Medicine, College of Medicine, National Taiwan University, Taipei 10002, Taiwan; [c]Department of Medical Research, National Taiwan University Hospital, Taipei 100, Taiwan

ABSTRACT **Vesicular trafficking involving SNARE proteins play a crucial role in the delivery of cargo to the target membrane. Arf-like protein 1 (Arl1) is an important regulator of the endosomal *trans*-Golgi network (TGN) and secretory trafficking. In yeast, ER stress-enhances Arl1 activation and Golgin Imh1 recruitment to the late-Golgi. Although Arl1 and Imh1 are critical for GARP-mediated endosomal SNARE-recycling transport in response to ER stress, their downstream effectors are unknown. Here, we report that the SNARE-associated protein Sft2 acts downstream of the Arl1–Imh1 axis to regulate SNARE recycling upon ER stress. We first demonstrated that Sft2 is required for Tlg1/Snc1 SNARE-recycling transport under tunicamycin-induced ER stress. Interestingly, we found that Imh1 regulates Tlg2 retrograde transport to the late-Golgi under ER stress, which in turn is required for Sft2 targeting to the late-Golgi. We further showed that Sft2 with 40 amino acids deleted from the N-terminus exhibits defective mediation of SNARE recycling and decreased association with Tlg1 under ER stress. Finally, we demonstrated that Sft2 is required for GARP-dependent endosome-to-Golgi transport in the absence of Rab protein Ypt6. This study highlights Sft2 as a critical downstream effector of the Arl1-Imh1 axis, mediating the endosome-to-Golgi transport of SNAREs.**

Monitoring Editor
Elizabeth Miller
MRC Laboratory of Molecular Biology

Received: Jan 23, 2023
Revised: Aug 7, 2023
Accepted: Aug 15, 2023

INTRODUCTION

Vesicular trafficking, a conserved mechanism regulating the proper transport of proteins, plays an essential role in maintaining cellular homeostasis and signaling (Tsvetanova, 2013; Tu *et al*., 2020). For proper vesicular transport, vesicles are first tethered to a target membrane before membrane fusion mediated by soluble NSF (N-ethylmaleimide-sensitive factor; SNARE) proteins (Bonifacino and Glick, 2004). Vesicle tethering requires tethering factors, including long-coiled coil proteins and multisubunit-tethering complexes, which not only contribute both specificity and efficiency to the fusion process but also directly mediate the action of SNAREs (Whyte and Munro, 2002; Hong and Lev, 2014; Wong *et al*., 2017).

Golgins, a family of long-coiled coil proteins found in the Golgi, work in concert with small GTPases, e.g., Arf-like proteins (Arls), for vesicle tethering (Munro, 2011; Witkos and Lowe, 2015; Yu and Lee, 2017). In yeast, Imh1 is the only GRIP-domain-containing Golgin, and it is recruited to the late-Golgi by Arl1 to be a downstream

This article was published online ahead of print in MBoC in Press (http://www.molbiolcell.org/cgi/doi/10.1091/mbc.E23-01-0019) on August 23, 2023.
Conflict of Interests: The authors declare no competing interests.
Author Contributions: C.-C.L. and F.S.L. designed the study and interpreted the results; C.-C. L. performed the majority of the experiments and analyzed the data; W.-Y. C. and Y.-T. C. contributed reagents/analytic tools and conducted the experiments; C.-C. L., and W.-Y. C. prepared the draft of the manuscript; C.-C. L., and F.S.L. wrote and edited the manuscript; and F.S.L. provided supervision, acquired funding, and performed project administration.
*Address correspondence to: Fang-Jen S. Lee (fangjen@ntu.edu.tw).
Abbreviations used: Arf, ADP-ribosylation factor; Arl, Arf-like protein; EE, early endosome; ER, endoplasmic reticulum; GARP, Golgi-associated retrograde protein; GEF, guanine nucleotide exchange factor; GFP, green fluorescent protein; GST, glutathione S-transferase; Lat-B, latrunculin B; mCh, mCherry; mRFP, monomeric red fluorescent protein; PM, plasma membrane; Rab, Ras-associated binding protein; Sft2, suppressor of sed5 ts 2; SNARE, soluble NSF (N-ethylmaleimide-sensitive factor); STX16, syntaxin 16; TGN, *trans*-Golgi network; TM, tunicamycin; t-SNARE, target SNARE; UPR, unfolded protein response; Vps, vacuolar protein sorting protein.

effector (Setty *et al.*, 2003; Yu and Lee, 2017). Mechanistically, Arf-GEF Syt1 activates Arl1 to form a ternary Arl1-Drs2-Gea2 complex that facilitates the Golgi localization of Imh1 (Tsai *et al.*, 2013). Although an increased abundance of Arl1 or golgin Imh1 can restore the defects of dysfunctional Ypt6 in endosome-to-Golgi trafficking of SNAREs (Chen *et al.*, 2019), the mechanism remains to be elucidated; specifically, how Golgin-mediated tethering coordinates with the fusion machinery through SNAREs is unclear.

The Golgi-associated retrograde protein (GARP) complex, a multisubunit-tethering complex, is required for retrograde transport from endosomes to the late-Golgi (Siniossoglou and Pelham, 2001; Bröcker *et al.*, 2010). The GARP complex comprises four subunits, Vps51/52/53/54, and is recruited to the late-Golgi via the interaction of Vps52 with Ypt6 (Siniossoglou and Pelham, 2001; Bonifacino and Hierro, 2011). The GARP complex interacts with the late-Golgi-localized SNAREs Tlg1/Tlg2 complex, which is known to mediate the fusion of endosome-derived vesicles with the late-Golgi in yeast; and similar results were found in mammals (Siniossoglou and Pelham, 2001; Pérez-Victoria and Bonifacino, 2009). Thus, the GARP complex has been proposed to promote the assembly of the SNARE complex and mediate fusion events (Pérez-Victoria and Bonifacino, 2009; Bonifacino and Hierro, 2011). Interestingly, a similar mechanism of vesicle fusion has been reported in which Ras-associated binding protein (Rab) protein Ypt7 recruits the heterohexameric homotypic fusion and vacuole protein sorting (HOPS) tethering complex to the vacuolar membrane, after which HOPS catalyzes the assembly of the vacuolar SNARE complex to form a partially zippered complex in the vacuolar fusion process (Song *et al.*, 2020; Torng *et al.*, 2020).

We previously reported that overexpression of Imh1 led to GARP complex recruitment to the late-Golgi in the absence of Ypt6 and abrogated the dysfunctional-retrograde transport of Tlg1/Snc1 SNAREs, suggesting the involvement of Imh1 in GARP-dependent SNARE recycling (Chen *et al.*, 2019). Our recent study demonstrated that when cells were under ER stress, the GARP complex was partially dysfunctional and needed the cooperation of Imh1 to maintain the proper localization of Tlg1/Snc1 SNAREs (Wang *et al.*, 2022). Given that SNAREs play vital roles in cells during ER- and proteostatic stress, we aim to investigate how the tethering protein Imh1 regulates SNARE transport under stress (Babazadeh *et al.*, 2019; Zhou *et al.*, 2020). Suppressor of sed5 ts 2 (Sft2) is a predicted tetra-spanning membrane protein in the late-Golgi, showing genetic interaction with Sed5 (Banfield *et al.*, 1995). Arl1 has been observed to colocalize extensively with Sft2, but only partially with a late-Golgi marker Sec7, suggesting that Arl1 and Sft2 are located in the same Golgi subcompartment (Liu *et al.*, 2005; Chen *et al.*, 2012). Notably, the exact function of Sft2 remains enigmatic. Previous study has shown that removal of both Sft2 and a conserved early-Golgi protein Got1 affects v-SNARE Snc1 recycling transport to the Golgi, indicating that Sft2 and Got1 have partially redundant roles in the fusion of vesicles with Golgi membranes (Conchon *et al.*, 1999). The fact that a single *sft2*Δ or *got1*Δ mutant does not affect Snc1 recycling transport has prompted us to identify a physiological condition under which Sft2 or Got1 is essential to SNARE recycling transport.

In this study, we found that Sft2 acted as a downstream regulator of the Arl1-Imh1 axis to facilitate Tlg1/Snc1 SNARE transport during tunicamycin (TM)-induced ER stress. We discovered that Imh1 needed Tlg2 to recruit Sft2 to the late-Golgi under ER stress. Furthermore, the N-terminus of Sft2 was essential for its function in regulating SNARE recycling transport after treatment with TM and proved to be important for enhancing the interaction of Tlg1 with Snc1. We also demonstrated that Sft2 was required for the Arl1–Imh1 axis to reverse Ypt6 dysfunction in SNARE recycling. Thus, our findings reveal a novel Arl1–Imh1 module that mediates SNARE-recycling transport under ER stress through sequential docking of Tlg2-Sft2-Tlg1 on the late-Golgi.

RESULTS

Sft2 is involved in the recycling transport of Tlg1/Snc1 SNAREs under TM-induced ER stress

To gain more insights into Sft2- and Got1-mediated SNARE recycling, we first examined whether Sft2 or Got1 is required for the proper localization of Snc1/Tlg1 SNAREs during ER stress. Consistent with a previous report (Conchon *et al.*, 1999), Snc1 and Tlg1 displayed proper localization at the plasma membrane (PM) and at the Golgi, respectively, in both *sft2*Δ and *got1*Δ cells under normal-growth conditions (Figure 1). However, Snc1/Tlg1 SNAREs exhibited mislocalization in *sft2*Δ cells under TM-induced stress, which is similar to that observed in *imh1*Δ cells (Figure 1). Interestingly, we observed that the recycling transport of Snc1, but not Tlg1, was defective in *got1*Δ cells under ER stress (Figure 1). Because these results suggested that Sft2 also participates in the transport of Snc1/Tlg1 SNAREs during ER stress, as the results observed in *arl1*Δ and *imh1*Δ cells in our previous study (Wang *et al.*, 2022), it raises a possibility that Sft2 is involved in the Arl1–Imh1 axis during ER stress.

Syt1–Arl1–Imh1 signaling regulates the recruitment of Sft2 to the late-Golgi upon ER stress

Previous studies showed Sft2 to be largely colocalized with Arl1 and Imh1 (Liu *et al.*, 2005; Chen *et al.*, 2010; Chen *et al.*, 2012; Hsu *et al.*, 2016). Consistent with this finding, we observed that Sft2 colocalized with Sec7 (late-Golgi marker), Arl1, and Imh1, indicating that Sft2 resided in close proximity to the Arl1–Imh1 axis in the late-Golgi (Supplemental Figure S1). We also found that under TM-induced stress, Sft2 colocalized with amplified puncta formed by Arl1–Imh1 proteins (Supplemental Figure S1; Hsu *et al.*, 2016). To determine whether Sft2 is regulated by the Arl1–Imh1 axis, we first determined the localization of Sft2 in *arl1*- or *imh1*-deleted cells. We observed that, similar to WT cells, Sft2 colocalized with the late-Golgi marker Sec7 in *arl1*Δ and *imh1*Δ cells under normal-growth conditions (Figure 2A). However, under ER stress, Sft2 was mislocalized in *arl1*Δ and *imh1*Δ cells (Figure 2A), and the expression of Arl1 or Imh1 restored Sft2 Golgi localization (Figure 2A). The first five amino acids, which are conserved, in the N-terminus of Imh1 have been shown to be critical for Imh1 function in mediating proper SNARE recycling during TM-induced ER stress (Wang *et al.*, 2022). We also found that Imh1^{dN5} (deletion of the first five amino acids) and Imh1^{F2A} (mutation of the most conserved second amino acid) failed to restore the localization of Sft2 in TM-induced *imh1*Δ cells, suggesting the importance of the Imh1 N-terminus for regulating Sft2 during ER stress (Figure 2B).

We previously reported that the UPR induced the phosphorylation of Arl1-GEF Syt1 at Ser416, which is necessary for the activation of Arl1 and the subsequent Golgi recruitment of Imh1 (Hsu *et al.*, 2016). To confirm whether UPR-triggered activation of the Syt1–Arl1–Imh1 axis is required for Golgi targeting of Sft2, we examined the localization of Sft2 in *syt1*Δ cells. Our results demonstrate that Syt1^{S416D}, but not Syt1^{S416A}, is able to restore the late-Golgi targeting of Sft2 in *syt1Δ* cells under TM-induced stress (Figure 2C), further showing that the observed mislocalization of proteins is not entirely due to defective glycosylation induced by TM.

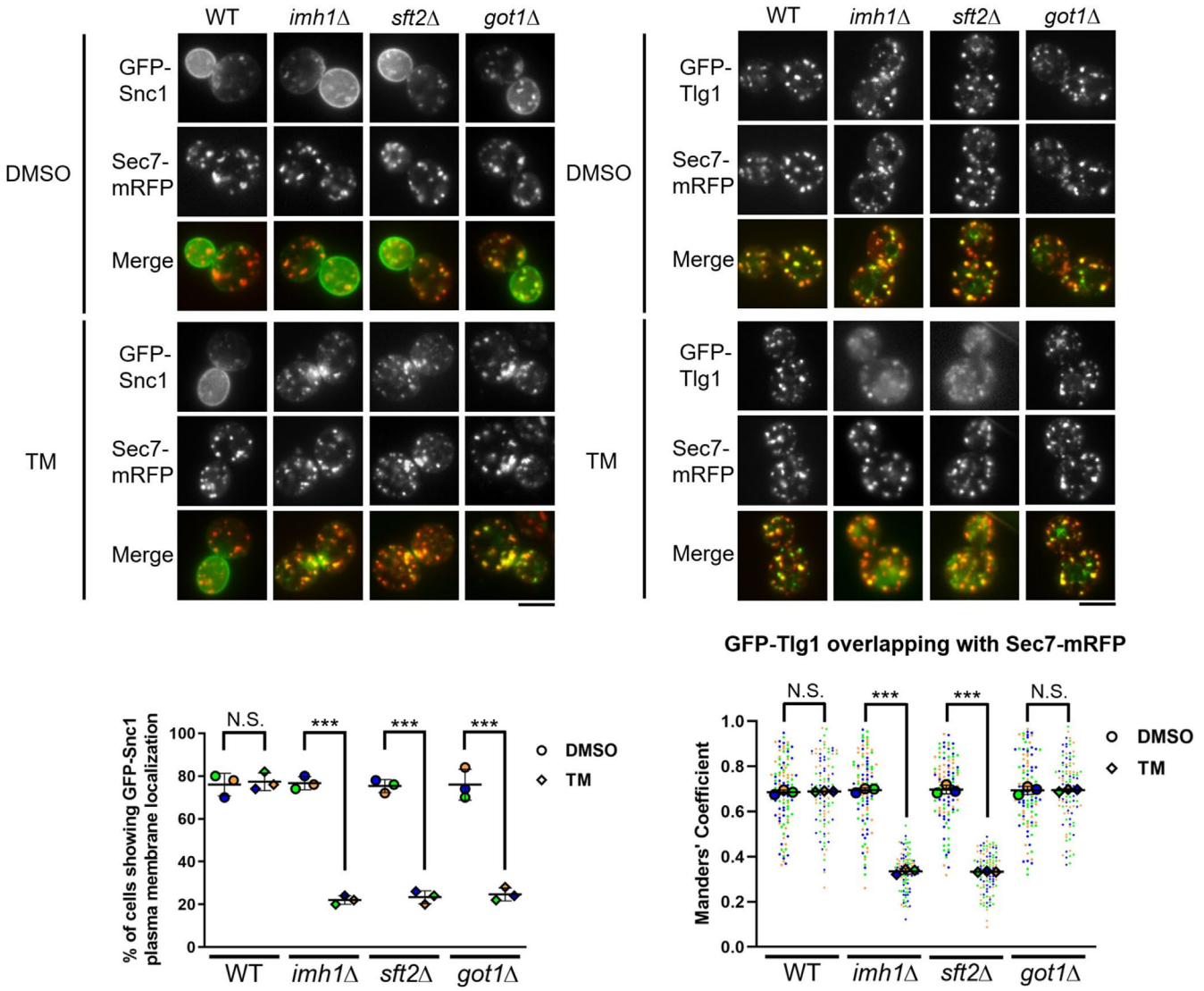

FIGURE 1: Sft2 is involved in the recycling transport of Tlg1/Snc1 SNAREs under ER stress. GFP-tagged Snc1 or Tlg1 was cotransformed with the late-Golgi marker Sec7-mRFP in the indicated cells. The yeast cells were cultured to the mid-log phase in selection medium and treated with DMSO or 1 μg/ml TM for 2 h before observation of live cells using fluorescence microscopy. Cells showing GFP-Snc1 PM signals were quantified ($N = 3$, $n = 100$) and analyzed by one-way ANOVA. The ratios of colocalization between GFP-Tlg1 and the late-Golgi marker Sec7-mRFP were quantified by using Manders' coefficient ($N = 3$, $n = 100$) and analyzed by one-way ANOVA. The analyzed data from three independent experiments are presented as the mean ± SD. ***$p < 0.001$; ns, not significant. Scale bar, 5 μm.

Imh1 and Sft2 interdependently mediate the proper localization of Tlg1/Snc1 SNAREs under ER stress

To characterize the role of Sft2 at the late-Golgi under ER stress, we sought to confirm that Sft2 mediates SNARE recycling in a similar manner to Imh1 under ER stress. We found that under TM-induced ER stress, deletion of *SFT2* phenocopied the mislocalization pattern of Tlg1/Snc1 SNAREs observed in *imh1*Δ cells (Figure 1). The intracellular compartments of GFP-Snc1 colocalized with the late-Golgi marker Sec7 in *sft2*Δ cells under ER stress (Figure 1). The accumulation of GFP-Snc1 in the late-Golgi suggested that anterograde-transport to the PM was defective; thus, we examined whether Sft2 is required for the anterograde transport of GFP-Snc1 under ER stress. To identify the defective phenotype of Snc1 in *sft2*Δ cells under ER stress, we treated the cells with latrunculin B (Lat-B), which inhibits endocytosis by preventing actin polymerization, after incubation with TM (Wang *et al.*, 2022). We found that, similar to the observations in *imh1*Δ cells, GFP-Snc1 localized to the PM in TM-treated *sft2*Δ and *got1*Δ cells after Lat-B incubation for 10 min (Supplemental Figure S2, A and B). This data indicates that the anterograde transport of Snc1 from the late-Golgi to the PM is perturbed, but not blocked, in the absence of Sft2 or Got1 during TM-induced ER stress.

To clarify that Sft2 affects SNARE recycling under ER stress, we first examined the colocalization of Arl1 and Imh1 in TM-treated *sft2*Δ cells and observed that Arl1 colocalized with Imh1 (Supplemental Figure S3A). Moreover, an increased number of Arl1 and Imh1 puncta were observed in response to TM treatment, suggesting that the activation of the Arl1–Imh1 axis was not altered in *sft2*Δ cells (Supplemental Figure S3A). Given that Imh1 cooperates with the GARP complex to facilitate SNARE-recycling transport during ER stress (Wang *et al.*, 2022), we wondered whether deletion of *SFT2* alters the localization of the GARP complex,

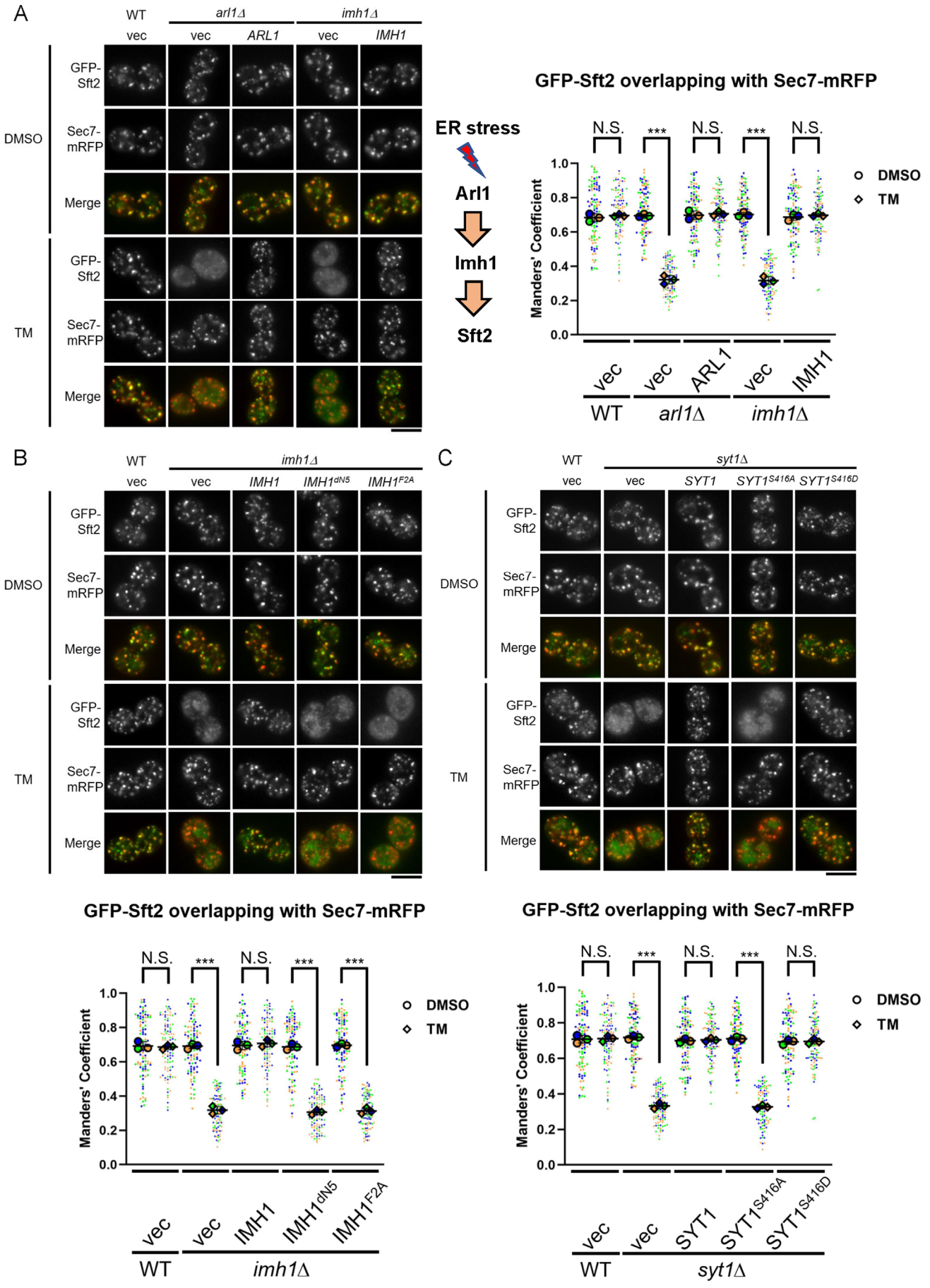
A
WT
arl1Δ
imh1Δ
vec
vec
ARL1
vec
IMH1
DMSO
TM
GFP-Sft2
Sec7-mRFP
Merge
ER stress
Arl1
Imh1
Sft2
GFP-Sft2 overlapping with Sec7-mRFP
Manders' Coefficient
N.S.
***
DMSO
TM
WT
arl1Δ
imh1Δ
B
imh1Δ
IMH1
IMH1dN5
IMH1F2A
C
syt1Δ
SYT1
SYT1S416A
SYT1S416D

thereby disrupting the transport of SNAREs under ER stress. We observed that the Golgi localization of the GARP complex was unaffected in TM-treated *sft2*Δ cells (Supplemental Figure S3B). We next examined the localization of GFP-Snc1 in *imh1*Δ or *sft2*Δ cells overexpressing Sft2 or Imh1, respectively. We further demonstrated that overexpression of Sft2 could not compensate for the loss of Imh1 during ER stress (Supplemental Figure S4). Altogether, our findings suggest that Sft2 functions downstream of Imh1, interdependently mediating the recycling of SNAREs upon ER stress.

Imh1 requires Tlg2 to mediate the localization and function of Sft2 under ER stress

SNAREs assemble into hetero-oligomeric bundles to exert their proper function. To clarify the mechanism of SNARE-recycling transport involved in the Imh1-Sft2 axis upon ER stress, we next sought to investigate the relevance between Sft2 and late-Golgi-localized SNAREs. Tlg2, a homologue of mammalian syntaxin 16 (STX16), has been reported to associate with the GARP complex and is involved in the assembly of the SNARE complex with Tlg1 and Vti1 at the late-Golgi (Holthuis *et al.*, 1998; Paumet *et al.*, 2001; Siniossoglou and Pelham, 2001; Gurunathan *et al.*, 2002; Reggiori *et al.*, 2003; Hong and Lev, 2014). We first confirmed the defects of Snc1 recycling to the PM in *tlg2*Δ cells. We then found that Snc1 colocalized with the late-Golgi marker Sec7 in *tlg2*Δ cells, and further showed that exocytosis of Snc1 was delayed (Supplemental Figures S5 and S6). In addition, consistent with a previous report (Holthuis *et al.*, 1998), the late-Golgi localization of Tlg1 was altered in *tlg2*Δ cells (Supplemental Figure S5). These results demonstrated that Tlg2 was required for the proper localization of Tlg1/Snc1 SNAREs. Considering this evidence, we speculated that Tlg2 might be involved in the Imh1–Sft2 axis. We examined the localization of Tlg2 in *imh1*Δ and *sft2*Δ cells and found that, during ER stress, GFP-Tlg2 became more diffuse in *imh1*Δ cells, but not in *sft2*Δ cells, suggesting that Imh1 but not Sft2 is needed for the proper localization of Tlg2 in this condition (Figure 3A). Interestingly, we found that Tlg2, but not Tlg1, was required for the late-Golgi localization of Sft2 under ER stress (Figure 3B). We previously showed that deletion of the first-five amino acids of Imh1 (Imh1^{dN5}) impaired Imh1 regulatory effects on the recycling of Tlg1 and its association with Tlg1 under ER stress (Wang *et al.*, 2022). Similarly, compared with wild-type Imh1, we found that Imh1^{dN5} showed a weakened association with Tlg2 under ER stress (Supplemental Figure S7). Altogether, our findings suggest that Imh1 regulates the Golgi targeting of these proteins in sequential steps under ER stress, as Sft2 requires Tlg2 for its late-Golgi localization to facilitate the recruitment of Tlg1, and Tlg1 in turn facilitates Snc1 exocytosis during TM-induced ER stress.

The N-terminus of Sft2 is required for mediating SNARE recycling under ER stress

We next sought to determine the functional domain that is necessary for Sft2 to perform its specific role under ER stress. Because both the N- and C-terminus of Sft2 are exposed to the cytosol (Conchon *et al.*, 1999; Bean *et al.*, 2017), we introduced truncated forms of Sft2, including Sft2^{dN40} (deletion of the first 40 amino acids), Sft2^{dN80} (deletion of the first 80 amino acids), and Sft2^{dC} (deletion of the last 22 amino acids), to examine whether these mutants can restore the defective transport of Tlg1/Snc1 SNAREs in TM-treated *sft2*Δ cells (Figure 4A). We found that Sft2^{dC}, but neither Sft2^{dN40} nor Sft2^{dN80}, restored the proper localization of Tlg1 and Snc1 in TM-treated *sft2*Δ cells (Figure 4B). We also observed that Sft2^{dN40} and Sft2^{dC} colocalized with Imh1 under ER stress (Figure 4C). However, Sft2^{dN80} failed to localize to the late-Golgi under both normal-growth conditions and TM-induced ER stress (Figure 4C). This data demonstrates the importance of the Sft2 N-terminal region for supporting Tlg1/Snc1 recycling transport under ER stress.

The N-terminus of Sft2 is critical for modulating interaction with Tlg1 under ER stress

Given that Sft2^{dN40} localized to the late-Golgi but failed to restore the transport of SNAREs under ER stress (Figure 4, B and C), we next examined whether Sft2^{dN40} is defective in the association with proteins in this pathway, namely the GARP complex, Imh1, Tlg2, and Tlg1. We performed coimmunoprecipitation (co-IP) assays with TM-treated cells and found that the association of full-length Sft2 with the GARP subunit Vps53, as well as Tlg1, was enhanced after TM treatment (Figure 5A). There was no significant difference in the association of Sft2 and Sft2^{dN40} with Vps53 in *sft2*Δ cells treated with or without TM (Figure 5A); however, compared with full-length Sft2, we found that Sft2^{dN40} showed a weaker association with Tlg1 under ER stress (Figure 5A). We further found that, compared with full-length Sft2, there was no significant difference in the association of Sft2^{dN40} with Imh1 in *sft2*Δ cells treated with or without TM (Figure 5B). In addition, similar to full-length Sft2, we found that Sft2^{dN40} remained associated with Tlg2 after TM treatment (Figure 5C). These data suggest that the first 40 amino acids in the N-terminus of Sft2 are critical for modulating its association with Tlg1 upon ER stress.

The N-terminus of Sft2 and the transmembrane domain of Tlg1 are important for modulating the interaction of Sft2, Tlg1, and Snc1

To clarify whether Sft2 is present in complex with Tlg1 SNARE, we first tested whether Sft2 can interact with Tlg1 in vitro. We found that Sft2 can be pulled down by purified GST-fused Tlg1, and this binding does not require the N-terminal 40 residues of Sft2 (Figure 6). Because Tlg1 is known to interact with v-SNARE Snc1

FIGURE 2: The Syt1–Arl1–Imh1 axis is required for the recruitment of Sft2 to the TGN upon ER stress. (A) Arl1–Imh1 axis is essential for the Golgi localization of Sft2 under TM treatment. The colocalization of GFP-Sft2 with the late-Golgi marker Sec7-mRFP was observed in *arl1*Δ or *imh1*Δ cells coexpressing Sec7-mRFP with an empty vector, Arl1 or Imh1 upon TM treatment. (B) The conserved N-terminal region of Imh1 is critical for Imh1 function in the recruitment of Sft2 under TM-induced conditions. GFP-Sft2 was coexpressed with Sec7-mRFP and different mutant forms of Imh1 in *imh1*Δ cells. (C) ER stress-induced phosphorylation of Syt1 at S416 is required for the proper localization of Sft2 under TM treatment. The colocalization of GFP-Sft2 with the late-Golgi marker Sec7-mRFP was observed in *syt1*Δ cells expressing Syt1, Syt1^{S416A}, or Syt1^{S416D}. (A–C) Yeast cells were cultured to mid-log phase in selection medium and treated with DMSO or 1 μg/ml TM for 2 h before observation of live cells using fluorescence microscopy. Scale bar, 5 μm. (A–C) The ratios of colocalization were determined by using Manders' coefficient to calculate the overlap of GFP-Sft2 with the late-Golgi marker Sec7-mRFP. The data from three independent experiments were analyzed ($N = 3$, $n = 100$) by one-way ANOVA and are presented as the mean ± SD. ***$p < 0.001$; ns, not significant.

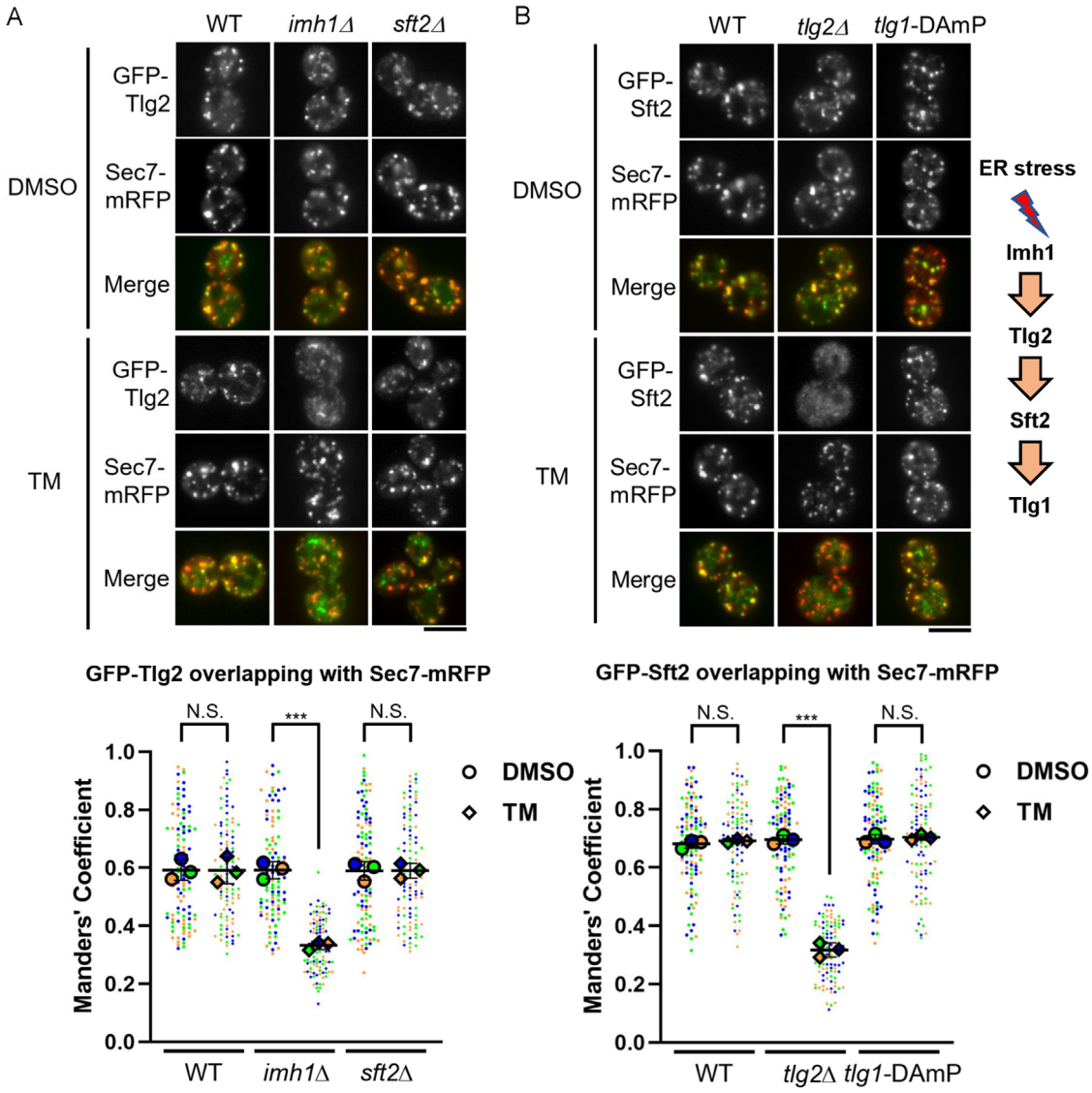

FIGURE 3: Tlg2 is involved in the recruitment of Sft2 to the late-Golgi through the regulation of Imh1 under ER stress. (A) The localization of Tlg2 is altered in *imh1*Δ cells, but not in *sft2*Δ cells under ER stress. GFP-Tlg2 was coexpressed with the late-Golgi marker Sec7-mRFP in the indicated cells. (B) Sft2 fails to localize to the late-Golgi in *tlg2*Δ cells but not in *tlg1*-DAmP cells (a *TLG1*-knockdown strain generated from BY4741) under ER stress. The localization of GFP-Sft2 was observed in the indicated cells expressing the late-Golgi marker Sec7-mRFP. (A and B) Yeast cells were cultured to mid-log phase in selection medium and treated with DMSO or 1 μg/ml TM for 2 h before observation of live cells using fluorescence microscopy. Scale bar, 5 μm. (A and B) The ratios of colocalization were determined by using Manders' coefficient to calculate the overlap of GFP-Tlg2 or GFP-Sft2 with the late-Golgi marker Sec7-mRFP. The data from three independent experiments were analyzed ($N = 3$, $n = 100$) by one-way ANOVA and presented as the mean ± SD. ***$p < 0.001$; ns, not significant.

(Holthuis *et al.*, 1998), we also examined whether Sft2 can affect the interaction of Tlg1 with Snc1. Interestingly, we found that GST-Tlg1 pulled down more Snc1 in the presence of an abundance of Sft2, but not $Sft2^{dN40}$, suggesting that the N-terminus of Sft2 is involved in the interaction between Tlg1 and Snc1. We next examined whether the C-terminal transmembrane domain of Tlg1 might be required for the interaction with Sft2 and Snc1. We found that the binding of Tlg1 to Sft2 or $Sft2^{dN40}$ and Snc1 was impaired by the absence of its transmembrane domain (Figure 6), suggesting that the transmembrane domain of Tlg1 is important for the function of the interaction region(s) in Tlg1.

Sec18 is the homologue of the mammalian NSF ATPase that catalyzes SNARE complex disassembly for the next round of vesicle fusion (Mayer *et al.*, 1996). At a nonpermissive temperature of 37°C, the ATPase activity of Sec18 is impaired, leading to accumulation of the SNARE complex in *sec18-1* cells (Holthuis *et al.*, 1998; Bryant and James, 2003). To determine whether Sft2 associates with the Tlg1 SNARE complex in vivo, we performed co-IP experiments in the temperature-sensitive *sec18–1* mutant. We found that the association of Snc1 with Tlg1 is significantly increased in *sec18-1* cells at the nonpermissive temperature (Supplemental Figure S8), whereas the association of Sft2 with Tlg1 is unchanged (Supplemental Figure S8), suggesting that Sft2 is not a member of the canonical-SNARE proteins. Overall, our in vivo and in vitro data suggest that under TM-induced ER stress, the N-terminus of Sft2 and the transmembrane domain of Tlg1 may contribute to the interaction

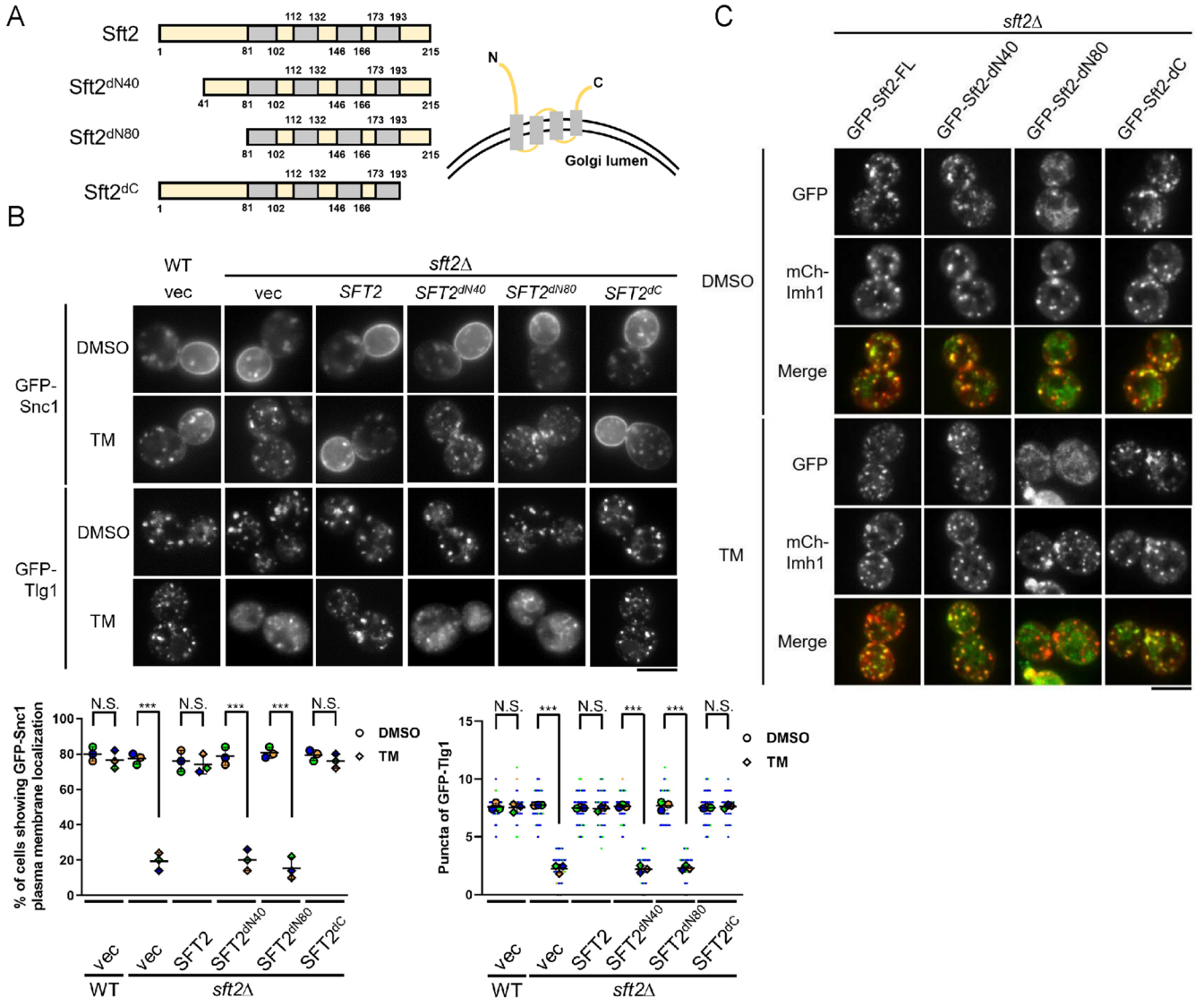

FIGURE 4: The N-terminal 40 amino acids of Sft2 are required for Sft2 function in mediating SNARE recycling under ER stress. (A) Schematic diagrams of Sft2 constructs with truncated mutants for dissecting the functional region(s). The light gray regions indicate the transmembrane domains of Sft2. (B) The N-terminal region of Sft2, but not the C-terminus of Sft2, is necessary for mediating SNARE transport under ER stress. GFP-tagged Snc1 or Tlg1 was coexpressed with the indicated truncated mutants of Sft2 in *sft2*Δ cells. Cells exhibiting the PM signals of GFP-Snc1 or the number of GFP-Tlg1 puncta were quantified ($N = 3$, $n = 100$) and analyzed by one-way ANOVA and unpaired *t* test, respectively. The analyzed data from three independent experiments are represented as the mean ± SD. ***$p < 0.001$; ns, not significant. (C) The N-terminal region of Sft2 is required for its late-Golgi localization. GFP-tagged truncation mutants of Sft2 were coexpressed with mCherry-Imh1 in *sft2*Δ cells. (B and C) Mid-log phase yeast cells were treated with DMSO or 1 μg/ml TM for 2 h before observation of live cells using fluorescence microscopy. Scale bar, 5 μm.

between Sft2 and Tlg1, which is critical for Tlg1/Snc1 recycling and modulating the Tlg1–Snc1 interaction.

Sft2 acts downstream of the Arl1–Imh1 axis to restore GARP-dependent endosome-to-Golgi transport in the absence of Ypt6

Ypt6, a homologue of mammalian Rab6, is critical for the recruitment of the GARP complex to the late-Golgi, mediating endosome-to-Golgi transport (Siniossoglou and Pelham, 2001). Our previous study demonstrated that the Ypt6 and Arl1-Imh1 axis function redundantly in endosome-to-Golgi trafficking (Chen *et al.*, 2019). Overexpression of Arl1 or Imh1 reestablished the recruitment of the GARP complex to the late-Golgi and abrogated the defective transport of Tlg1/Snc1 SNAREs in the absence of Ypt6 (Chen *et al.*, 2019). To better understand the role of Sft2 in downstream of Arl1–Imh1 signaling, we utilized a model in which either Arl1 or Imh1 was overexpressed in *ypt6*Δ cells to examine the importance of Sft2 under different cellular conditions. We found that similar to the observed effects of Arl1 and Imh1 (Benjamin *et al.*, 2011), Sft2 failed to exhibit proper Golgi localization in the absence of Ypt6, but this localization was restored by overexpressing Arl1 or Imh1 (Figure 7, A and B). Interestingly, high-copy amplification of Arl1 or Imh1 failed to restore the localization of Snc1 (Figure 7C) or suppress high-temperature growth defects in *ypt6sft2*Δ cells (Figure 7D). However, the Arl1–Imh1 axis restored the localization of the GARP complex in the absence of both Ypt6 and Sft2 (Figure 7C). Our observations

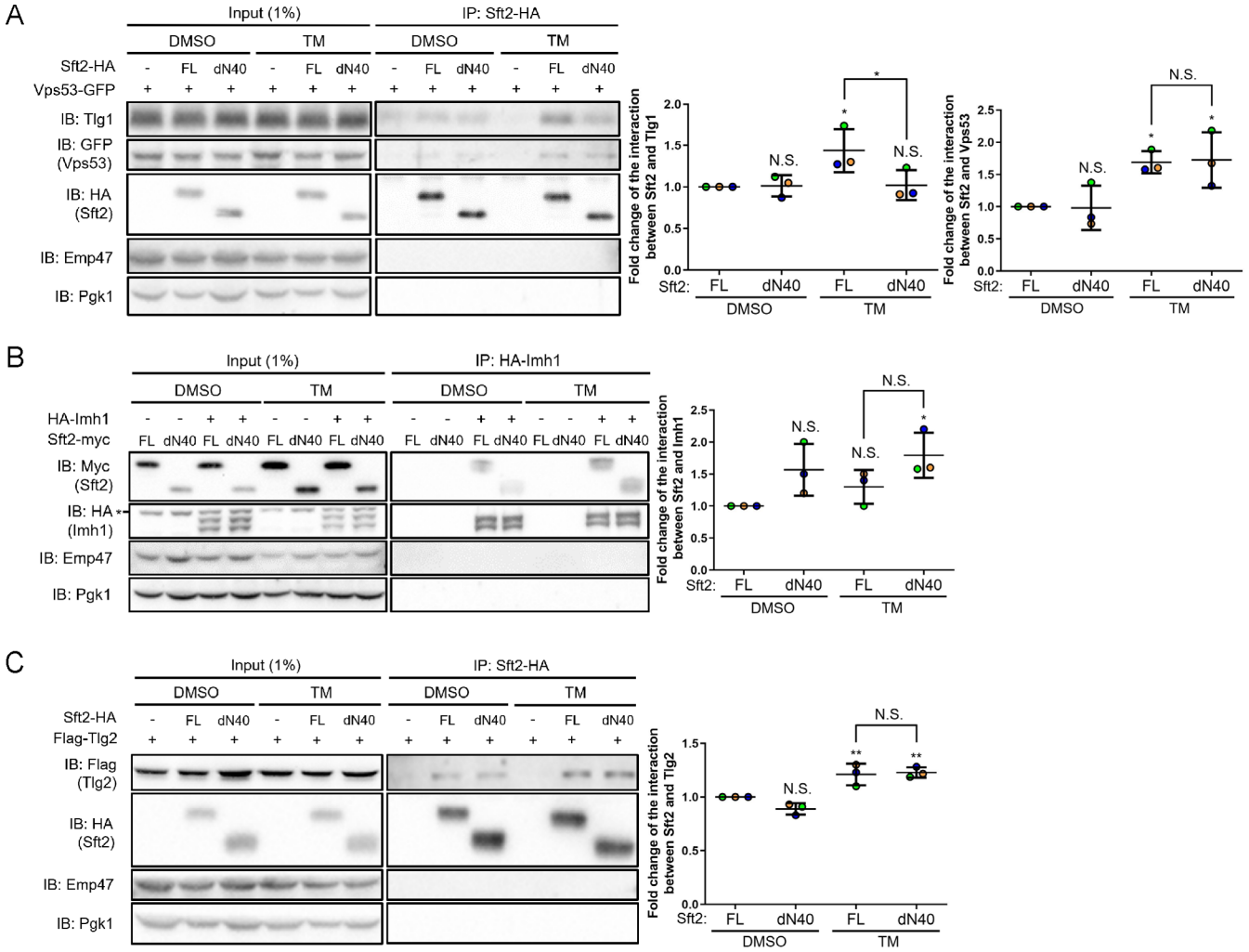

FIGURE 5: The N-terminal 40 amino acid-deleted Sft2 decreases its association with Tlg1, but not Vps53, Imh1, or Tlg2 under ER stress. (A) The N-terminal 40 amino acids of Sft2 are critical for regulating its association with Tlg1 but not Vps53 upon TM-induced stress. Vps53-GFP was coexpressed with $Sft2^{FL}$-HA or $Sft2^{dN40}$-HA in *sft2*Δ cells.(B) The first 40 amino acids at the N-terminus of Sft2 are not required for Sft2 association with Imh1. Yeast cells were cotransformed with HA-Imh1 and $Sft2^{FL}$-myc or $Sft2^{dN40}$-myc. (C) The first 40 amino acids at the N-terminus of Sft2 are not required for its association with Tlg2. Flag-Tlg2 was coexpressed with $Sft2^{FL}$-HA or $Sft2^{dN40}$-HA in *sft2*Δ cells. (A–C) The indicated cells were treated with TM for 2 h and further incubated with 3 mM crosslinker DSP for 30 min before the preparation of cell lysates and co-IP assays. The bound-protein complexes were analyzed using western blotting. Asterisk indicated the nonspecific bands. The intensities of bound proteins were measured by ImageJ Fiji software and the signals were normalized to the input and HA-tagged proteins. The analyzed data from three independent experiments are represented as the mean ± SD after analysis via one-way ANOVA. *$p < 0.05$; **$p < 0.005$; ns, not significant.

indicated that Sft2 is required for the Arl1–Imh1 axis to suppress the defects resulting from Ypt6 dysfunction, even though the GARP complex exhibited normal distribution. Nevertheless, overexpression of Sft2, in contrast to Imh1, failed to restore the PM localization of Snc1 in *ypt6*Δ cells (Supplemental Figure S9A). We also observed that overexpression of Sft2 failed to reestablish the proper localization of Arl1 and Imh1 in *ypt6*Δ cells (Supplemental Figure S9B). Our data demonstrated that Sft2 acts as a downstream regulator of the Arl1–Imh1 axis to restore endosome-to-Golgi transport in the absence of Ypt6. Altogether, this study reveals that Sft2 plays a critical role downstream of Arl1–Imh1 signaling.

DISCUSSION

The cooperative actions of golgins and SNAREs ensure the specificity of vesicle trafficking in tethering and fusion in a spatiotemporally regulated manner. Previous studies have shown that genes involved in the secretory pathway are upregulated under ER stress, providing valuable mechanistic insights into the contribution of vesicle trafficking to alleviate ER stress (Travers *et al.*, 2000; Tsvetanova, 2013). In this study, we discovered that the SNARE-associated protein Sft2 functions downstream of golgin Imh1 to regulate SNARE recycling transport during ER stress. Our findings expand the molecular mechanism underlying the cooperation between the tethering factor golgin and SNAREs in the secretory pathway upon ER stress.

We have previously shown that ER stress upregulates the activation of the Arl1–Imh1 axis through Ire1-dependent phosphorylation of the Arl1-GEF Syt1 (Hsu *et al.*, 2016). Moreover, under ER stress, golgin Imh1 was identified to be phosphorylated by mitogen-activated protein kinase Slt2/ERK2, which is required for Tlg1/Snc1 SNAREs recycling transport (Wang *et al.*, 2022). Imh1 is required for

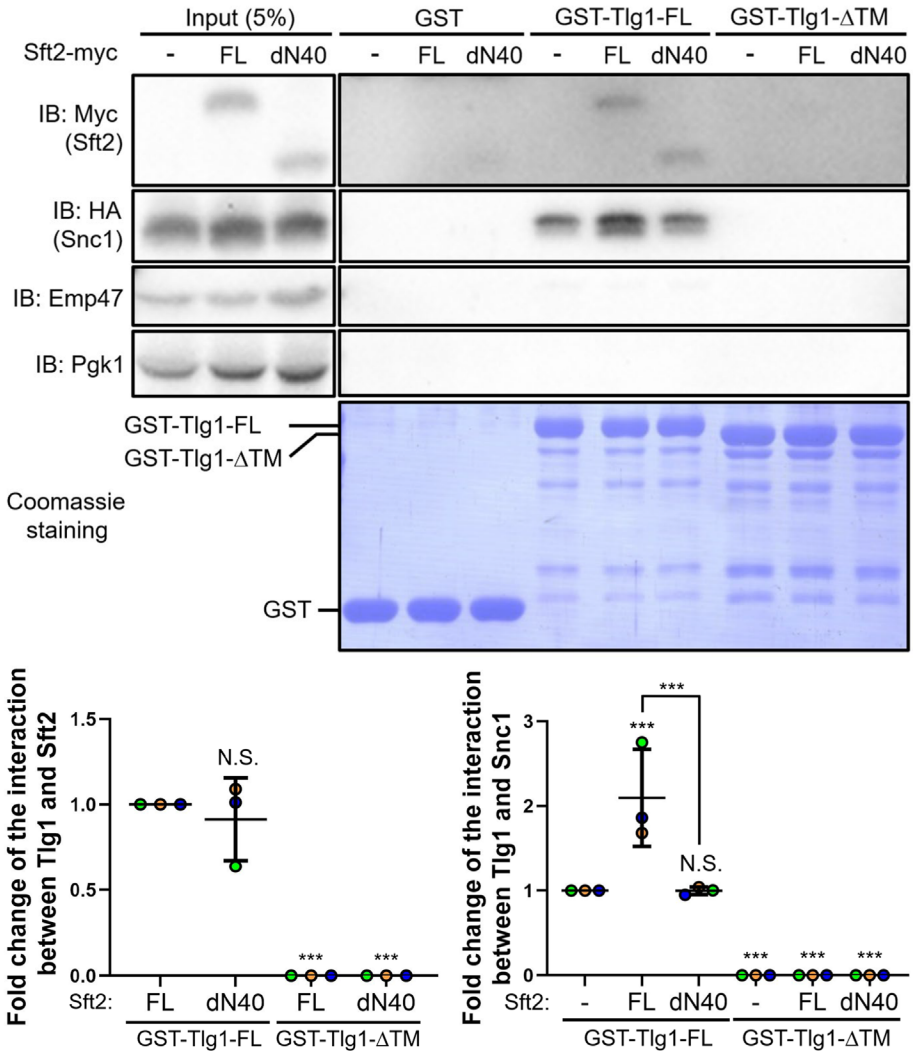

FIGURE 6: The N-terminus of Sft2 and the transmembrane domain of Tlg1 are important for modulating the interaction of Sft2, Tlg1, and Snc1. The N-terminal 40 amino acid-deleted Sft2 is able to associate with Tlg1 but fails to modulate the interaction of Tlg1 with Snc1. The transmembrane region of Tlg1 contributes to its association with Sft2 and Snc1. Cell lysates were collected from *sft2*Δ cells coexpressing $Sft2^{FL}$-myc or $Sft2^{dN40}$-myc with HA-Snc1 and incubated with purified GST-Tlg1 or GST-Tlg1 lacking the transmembrane region (GST-Tlg1-ΔTM; amino acids 1–206) at 4°C for 1 h. The bound proteins were analyzed by western blot using indicated antibodies. The intensities of bound $Sft2^{FL}$-myc, bound $Sft2^{dN40}$-myc, and bound HA-Snc1 were measured by ImageJ Fiji software. The bound signals were normalized to the respective input and GST-tagged proteins. The analyzed data from three independent experiments are represented as the mean ± SD after analysis via one-way ANOVA. ***$p < 0.001$; ns, not significant.

the recycling of early endosome (EE)-derived vesicles carrying Tlg1, but not late endosome (LE)-derived vesicles carrying Snc1, to the late-Golgi under ER stress (Wang *et al.*, 2022). Deletion of both Sft2 and Got1 has been previously shown to impair the recycling transport of Snc1 (Conchon *et al.*, 1999). Interestingly, our data show that under ER stress, deletion of Sft2 or Got1 alone is sufficient to trap Snc1 at the late-Golgi and delay exocytic transport of Snc1 to the PM. However, Sft2, but not Got1, is required for the retrograde transport of Tlg1 to the late-Golgi upon ER stress (Figure 1). Given that Tlg1 is mislocalized in *sft2*Δ cells under ER stress, Sft2, similar to Imh1, engages in the transport of Tlg1 from EEs to the late-Golgi. Consistently, Sft2 has been reported to be involved in the retrograde transport of ricin toxin A from EEs to the *trans*-Golgi network (TGN) in a route different from that of retromer and Snx4 (Becker *et al.*, 2016). These results indicate that Sft2 and Got1 mediate different factors in the Golgi complex to regulate Snc1 exocytic transport from the late-Golgi to the PM under ER stress.

Notably, previous studies have suggested that two late-Golgi t-SNAREs, Tlg1 and Tlg2, are required for the recycling of Snc1 from endosomes to the Golgi (Holthuis *et al.*, 1998; Lewis *et al.*, 2000). Moreover, the localization of Tlg1 is disrupted in *tlg2*Δ cells (Holthuis *et al.*, 1998). Tlg2 is involved in the GARP-dependent assembly of the SNARE complex with Tlg1 and Vti1 at the late-Golgi (Holthuis *et al.*, 1998; Paumet *et al.*, 2001; Siniossoglou and Pelham, 2001; Gurunathan *et al.*, 2002; Reggiori *et al.*, 2003; Hong and Lev, 2014). We recently found that in the absence of Tlg1, Snc1 accumulates at the late-Golgi, which leads to delayed exocytosis (Wang *et al.*, 2022). Similarly, Snc1 accumulates at the late-Golgi in *tlg2*Δ cells, delaying its exocytosis (Supplemental Figures S5 and S6). Interestingly, Golgin-97, a homologue of yeast Imh1, has been demonstrated to capture STX16-containing vesicles, which is required before STX16-mediated fusion (Lu *et al.*, 2004; Shin *et al.*, 2020). Similar to these observations, we noticed that during ER stress, Imh1 is required for the late-Golgi localization of Tlg2. Moreover, Tlg2 facilitates Golgi targeting of Sft2 to mediate the retrograde transport of Tlg1 to the late-Golgi under ER stress (Figure 4B). Therefore, our findings reveal a sequential recruitment event in which Imh1 directs the localization of Tlg2, Sft2, and Tlg1 to the late-Golgi. Studying golgin GM130 at the *cis*-Golgi, Lowe's group reported that GM130 interacted with syntaxin 5 to couple-membrane tethering and fusion, allowing the Sed5-containing *trans*-SNARE complex assembly in close proximity (Diao *et al.*, 2008). Our data reveal a similar Imh1 action at the late-Golgi, implying that Imh1 might mediate TGN-SNARE-complex assembly to change membrane trafficking under ER stress. Further biochemical studies are needed to understand how Sft2 precisely functions in SNARE-recycling transport.

Previous studies from Glick's group proposed that Golgi-cisternal maturation can be divided into three successive stages: 1) *cis*-Golgi cisternae, 2) medial- and *trans*-Golgi cisternae, and 3) carrier formation at the TGN (Day *et al.*, 2013; Papanikou and Glick, 2014). Recently, Nakano's group suggested that the TGN stage can be further divided into two substages: the "early TGN" that receives recycling traffic from endosomes and the "late TGN" that produces carriers for transport to the PM (Tojima *et al.*, 2019). Their studies suggest that recycling of proteins from endocytic compartments into

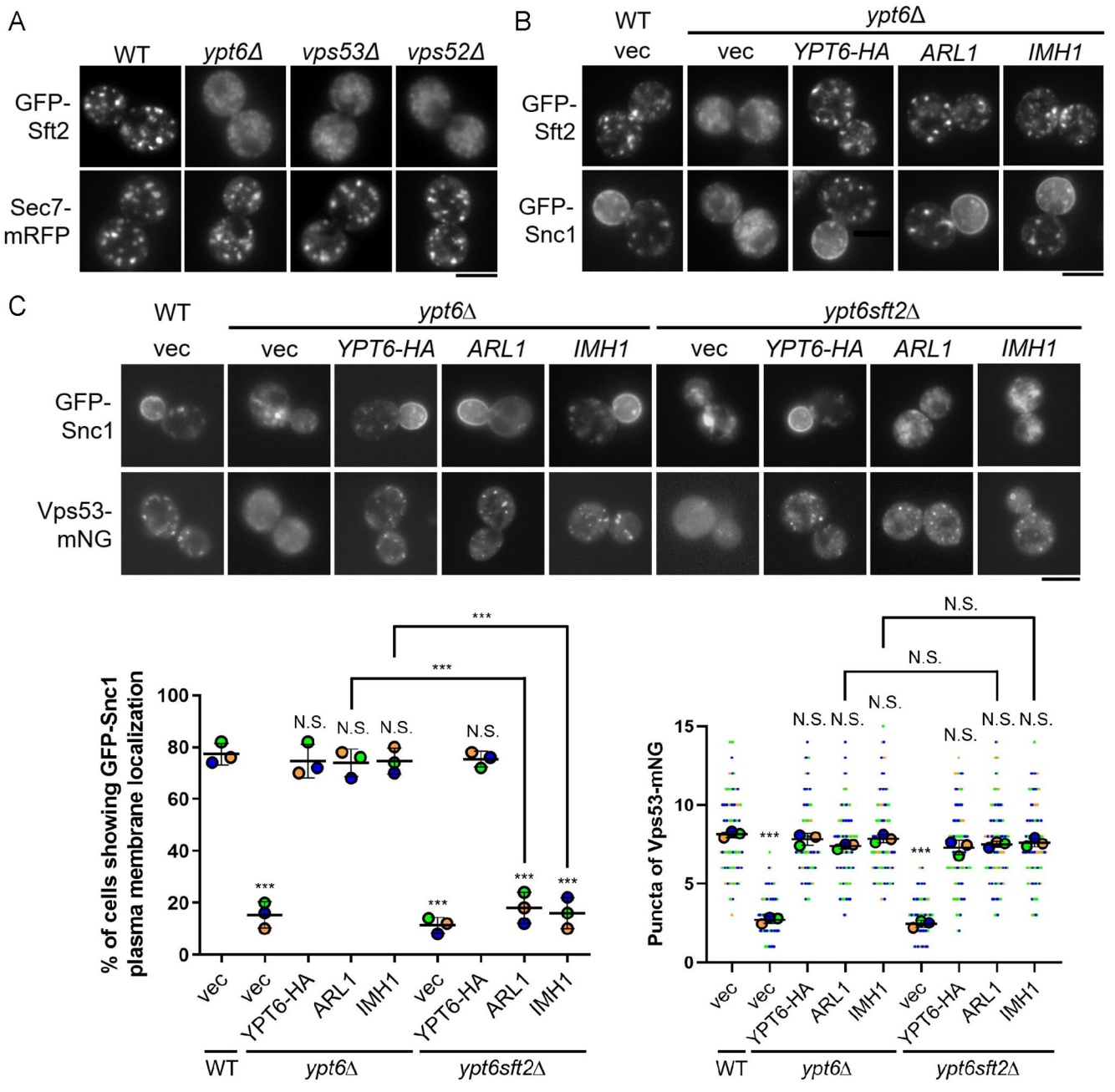
A
WT
ypt6Δ
vps53Δ
vps52Δ
GFP-Sft2
Sec7-mRFP
B
WT
vec
ypt6Δ
vec
YPT6-HA
ARL1
IMH1
GFP-Sft2
GFP-Snc1
C
WT
vec
ypt6Δ
vec
YPT6-HA
ARL1
IMH1
ypt6sft2Δ
vec
YPT6-HA
ARL1
IMH1
GFP-Snc1
Vps53-mNG
% of cells showing GFP-Snc1 plasma membrane localization
Puncta of Vps53-mNG
N.S.
***
WT
ypt6Δ
ypt6sft2Δ
D
30˚C
37˚C
WT/vec
ypt6Δ
vec
ARL1
IMH1
ypt6sft2Δ
vec
YPT6-HA
ARL1
IMH1

the "early TGN" (or *trans*-Golgi) depends on the Ypt6-dependent GARP complex; and then the "early TGN" receives recycling proteins and undergoes cisternal maturation to the "late TGN", thereby producing different transport carriers for exocytosis. Previous studies have shown that an early TGN transmembrane protein, Sys1, is required for Arl3 function in Arl1 recruitment; and Arl1, in turn, recruits the golgin Imh1 (Behnia *et al.*, 2004; Setty *et al.*, 2004). Arl1 is also involved in recruitment of the late TGN Sec7 (McDonold and Fromme, 2014) and mammalian Arl1 was reported to recruit GEF BIG1/2, mammalian homologues of Sec7 (Christis and Munro, 2012). In addition, mammalian homologues of Imh1, such as Golgin 97, are known to function as a tether that captures endosome-derived vesicles to promote their fusion with the TGN membrane (Munro, 2011), implicating a possible function of a Sys1-Arl3-Arl1-Imh1 signaling cascade in endosome-to-TGN trafficking in yeast (Behnia *et al.*, 2004; Setty *et al.*, 2004; Yu and Lee, 2017). The Glick lab found that Tlg1 consistently arrived at the TGN before Sec7 and departed before Sec7 (Day *et al.*, 2018). A study from Nakano's lab showed that Sys1 and Ypt6 accumulate before Tlg2 and Sec7 (Tojima *et al.*, 2019). Their observation that Sys1 appeared before Tlg2 is consistent with the idea that the Sys1–Arl3–Arl1–Imh1 axis and Sft2 are involved in capturing endosome-derived vesicles to target them to the early TGN for Tlg2-Tlg1-mediated membrane fusion, which is critical for receiving retrograde cargos, such as Snc1, required for late TGN function.

The N-terminal cytosolic domain of Sft2 is required for mediating the late-Golgi targeting of Tlg1 in TM-treated cells. The enhanced association of Tlg1 and Sft2 in TM-induced cells apparently occurs in a manner dependent on the state of the N-terminus of Sft2. Interestingly, we also found that the C-terminal transmembrane domain of Tlg1 is required for Tlg1-Sft2 interaction in vitro. We speculate that TM-induced ER stress may alter the conformation of Tlg1 and/or the cytosolic N-terminal region of Sft2, leading to enhanced Sft2-Tlg1 association for the Tlg1-Snc1 interaction and Tlg1/Snc1 recycling. In addition, several residues at the N-terminus of Sft2 have been found to be posttranslationally modified (Zielinska *et al.*, 2012; Lanz *et al.*, 2021; Zhou *et al.*, 2021). These modifications of the N-terminus of Sft2 may also contribute to the function of Sft2 in Tlg1/Snc1 recycling. Further analysis of these modifications is needed to better understand how Sft2 is regulated and functions in response to TM-induced stress.

The SNARE complex generally comprises three or four SNARE proteins that form four helical bundles as a core complex to mediate membrane fusion (Yoon and Munson, 2018). After fusion, the SNARE complex is disassembled by Sec18 ATPase (Mayer *et al.*, 1996). Our data showed that Sft2 associates with SNARE proteins but Sec18 may not regulate this association. Previous studies have proposed an elegant model for the interaction between the tether golgin and the SNARE proteins (Diao *et al.*, 2008; Ganley *et al.*, 2008) that could catalyze SNARE assembly via modulation of the Rab protein. Pfeffer's group found that Rab6 competes for interaction of golgin GCC185 with STX16, which in turn releases SNARE proteins from the tether-SNARE complex to drive membrane fusion (Ganley *et al.*, 2008). We speculate that Sft2 may be involved in the association of Imh1 with Tlg1 and direct the Tlg1-containing SNARE complex to the vicinity of Imh1, which modulates SNARE proteins to a specific membrane-microdomain, thereby promoting membrane fusion. Although our data suggest that Sft2, like Imh1, is involved in the efficient packaging of Snc1 into exocytic vesicles under ER stress, it is also possible that Snc1 vesicles can tether to the late-Golgi (early TGN) but cannot fuse efficiently in *sft2*Δ or *imh1*Δ cells. Functional characterization of the Imh1-Sft2-SNARE interaction will be important for further studies.

During ER stress, some misfolded proteins may escape the ER and be disposed of in the post-ER secretory pathway for delivery to the lysosome/vacuole (Sun and Brodsky, 2019; Schwabl and Teis, 2022). It has been reported that misfolded glycosylphosphatidylinositol-anchored proteins are transported to the Golgi upon ER stress, and then transiently reach the cell surface before being transported endocytically to lysosomes for degradation (Satpute-Krishnan *et al.*, 2014). Previous study showed that deletion of both Snc1 and Snc2 results in defective post-Golgi transport of secretory proteins (Protopopov *et al.*, 1993). Therefore, we propose that it is important for the Arl1–Imh1–Sft2 axis to maintain recycling of Snc1 SNARE during ER stress for exocytosis of proteins, which contributes to the alleviation of ER stress.

The GARP complex requires Ypt6 to be localized at the Golgi and is profoundly involved in Snc1 and Tlg1 recycling to the late-Golgi (Siniossoglou and Pelham, 2001; Chen *et al.*, 2019). Our previous study showed that overexpression of Arl1 or Imh1 restored GARP localization at the late-Golgi in *ypt6*Δ cells and subsequently rescued the retrograde transport of Tlg1/Snc1 SNAREs to the late-Golgi (Chen *et al.*, 2019). In this study, we found that overexpression of Imh1 did not require Sft2 to restore GARP localization in *ypt6sft2*Δ cells but needed it to rescue Snc1 transport to the late-Golgi (Figure 7C). This result supports the supposition that Sft2 acts downstream of the GARP complex to facilitate the recycling transport of Tlg1/Snc1. Further studies are needed to improve our understanding of the mechanism underlying how Sft2 physically engages in the regulation of Imh1-mediated SNARE recycling under ER stress.

Overall, our findings led us to propose the following model for expanding the mechanism of SNARE-recycling transport upon ER

FIGURE 7: Sft2 is involved in the suppression of the Arl1–Imh1 axis in the absence of Ypt6. (A) Ypt6 and the GARP complex are required for Golgi localization of Sft2. The indicated-yeast cells were transformed and expressed with fluorescently tagged Sft2 or Sec7. (B) Overexpression of Arl1 or Imh1 restores the localization of Sft2 and Snc1 in *ypt6*Δ cells. Localization of GFP-tagged Sft2 or Snc1 was observed in *ypt6*Δ cells overexpressing Arl1 or Imh1. (C) The Arl1–Imh1 axis and Sft2 act interdependently to cooperate with the GARP complex to suppress the Snc1 transport defect under conditions of Ypt6 dysfunction. GFP-Snc1 or Vps53-mNG was coexpressed with vector, Ypt6-HA, Arl1, or Imh1 in WT, *ypt6*Δ, or *ypt6sft2*Δ cells. The cells that exhibited GFP-Snc1 PM signals or the number of Vps53-mNG puncta were quantified ($N = 3$, $n = 100$) and analyzed by one-way ANOVA. Analyzed data from three independent experiments are presented as mean ± SD. ***$p < 0.001$; ns, not significant. (A–C) The indicated-yeast cells were cultured to mid-log phase in selection medium and live cells were observed using fluorescence microscopy. Scale bar, 5 μm.
(D) Overexpression of the Arl1–Imh1 axis failed to suppress temperature-sensitive growth defects in *ypt6sft2*Δ cells. The indicated strains transformed with vector, Ypt6-HA, Arl1, or Imh1, were serially diluted 10-fold and spotted on selection plates lacking *URA*. The plates were incubated at 30°C or 37°C before imaging.

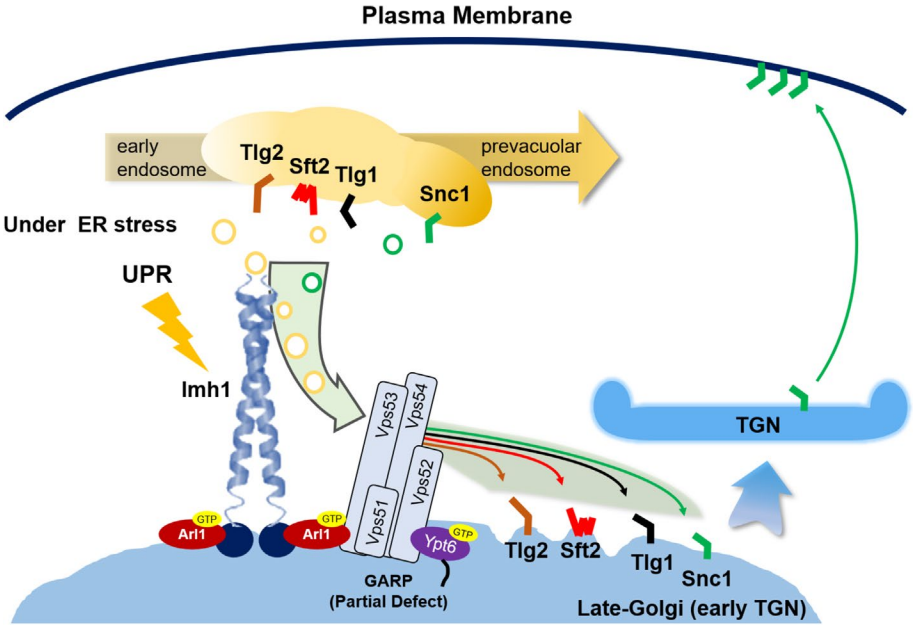

FIGURE 8: Model of the Arl1–Imh1–Tlg2–Sft2–Tlg1 cascade for SNARE-retrograde transport under ER stress. During TM-induced ER stress, the UPR triggers the activation of the Arl1–Imh1 pathway at the late-Golgi (early TGN) to cooperate with the partially defective GARP complex. Imh1 requires Tlg2 for the recruitment of Sft2 such that it is in close proximity to coordinate with the GARP complex and thus maintain the proper transport of Tlg1/Snc1 SNAREs.

stress (Figure 8). Under normal conditions, the Ypt6-mediated GARP complex is sufficient to maintain endosome-to-TGN retrograde transport, which allows Tlg1/Snc1 SNAREs to reach their proper distributions. However, when cells encounter ER stress, cooperation between the Arl1–Imh1 axis and GARP complex is needed to recruit Tlg2 and Sft2 to the late-Golgi (early TGN). Imh1 requires Tlg2 to facilitate the recruitment of Sft2, which subsequently mediates the recycling of Tlg1-containing vesicles from EEs to the late-Golgi. Therefore, Snc1 can be effectively transported to the PM through the late-Golgi. The N-terminal deletion of Sft2 weakens the association between Sft2 and Tlg1 and, therefore, the proper localization of Tlg1/Snc1 SNAREs from EEs cannot be restored, suggesting the functional importance of the Sft2 N-terminal region for Tlg1 docking or fusion to the late-Golgi (early TGN).

In conclusion, we identified a role for Sft2 downstream of the Arl1–Imh1 axis in regulating Tlg1/Snc1 SNAREs recycling transport under ER stress. Our study reveals a possible mechanism of endosome-to-Golgi retrograde transport through sequential docking of Tlg2-Sft2-Tlg1 upon ER stress, in which Sft2 acts as a newly discovered intermediary. How Sft2 contributes to the Imh1-dependent endosome-to-Golgi retrograde transport pathway under ER stress remains to be investigated. Further analysis of the biochemical properties of Sft2 will allow us to better understand the detailed mechanism of Sft2-mediated retrograde transport under ER stress.

MATERIALS AND METHODS

Yeast strains, plasmids, and antibodies

Supplemental Tables S1 and S2 list detailed information on the yeast strains and plasmids used in this study, respectively. The transformation of yeast was achieved via the lithium-acetate method (Ito *et al.*, 1983). The plasmids were cloned based on standard protocols (Sambrook and Russell, 2001).

For western blotting, the following primary antibodies were used with the noted dilutions: anti-GFP (1:3000), anti-Tlg1 (1:5000), anti-Emp47 (1:5000), anti-Pgk1 (1:3000), anti-Flag (1:5000), anti-HA (1:5000, Covance Inc.), and anti-Myc (1:3000, #2276S, Cell-Signaling Technology). The secondary antibody was goat horseradish peroxidase (HRP)-conjugated anti-rabbit/mouse IgG (1:5000, NA934 V/NA931 V, GE Healthcare). To avoid interference from denatured IgG, the VeriBlot for IP detection reagent (HRP) (ab131366, Abcam) was used as the secondary antibody for the protein-interaction analysis. Anti-GFP, anti-Tlg1, anti-Emp47, anti-Pgk1, and anti-Flag antibodies were generated in our laboratory as previously described (Chen *et al.*, 2019; Wang *et al.*, 2022). *Oryctolagus cuniculus* (female New Zealand white rabbits) were immunized with purified *Escherichia coli*-expressed recombinant protein. All animal experiments were approved by the Institutional Animal Care and Use Committee (IACUC) and performed in accordance with the institutional guidelines of the IACUC, National Taiwan University.

Microscopy and fluorescent image analysis

For the observations of live cells expressing fluorescent-fusion proteins, transformed yeast cells were cultured to the mid-log phase in appropriate synthetic medium with 2% (wt/vol) glucose. Mid-log phase cells were treated with DMSO (control treatment; D5879, Sigma-Aldrich) or 1 μg/ml TM (#654380, Sigma-Aldrich) for 2 h at 30°C to induce the UPR as described in our previous studies (Wang *et al.*, 2022). After DMSO or TM treatment, cells were mounted on glass slides immediately for observation at room temperature. Treatment with Lat-B (#428020, Sigma-Aldrich) was performed as described in our recent study (Wang *et al.*, 2022). Yeast cells coexpressing GFP-Snc1 and Sec7-mRFP were cultured to the mid-log phase and treated with 1 μg/ml TM for 2 h at 30°C. After treatment with TM for 2 h, 100 μM Lat-B was added to block endocytosis of Snc1. Yeast cells were harvested at different time points and immediately imaged by microscopy. Images of live cells were captured with an Axioplan microscope (Carl Zeiss, Thornwood, NY) equipped with a Plan-Apochromat 100×/1.4 objective lens, a Cool Snap FX camera, and Axio Vision Rel software. The multichannel images were merged using Axio Vision Rel software. All microscopy images of each sample within an experiment were captured with identical-exposure times and image-processing procedures. The ratio of cells with PM signals was examined as described in previous studies (Hankins *et al.*, 2015; Xu *et al.*, 2017; Chen *et al.*, 2019). The signals of fluorescent-fusion proteins were detected with ImageJ Fiji software as previously reported (Chen *et al.*, 2019; Wang *et al.*, 2022).

Protein interaction analysis

To analyze the interaction between Sft2 and its associated proteins in yeast, *sft2Δ* cells were cotransformed with appropriately tagged Sft2 with Vps53-GFP, HA-Imh1, or Flag-Tlg2. The following procedures were performed as described in previous studies (Siniossoglou and Pelham, 2001; Wang *et al.*, 2022). Yeast cells were cultivated to the

mid-log phase in synthetic drop-out medium for 14 h and subsequently treated with DMSO or 1 μg/ml TM for 2 h at 30°C. Seventy OD_{600} of cells were harvested and washed with 1 ml of 20 mM NaN_3 and NaF. Spheroplasts were generated as previously described (Wang *et al.*, 2022). Cells were treated with Zymolyase-100T (#120493, Ambio) and 1% β-mercaptoethanol in K-Pi buffer (190 mM K_2HPO_4, 310 mM KH_2PO_4, and 1.2 M sorbitol in ddH_2O) on an end-over-end rotator at 12 rpm at 30°C for 1 h. The spheroplasts were washed three times with 1 ml K-Pi buffer and then subjected to 3 mM dithiobis (succinimidyl propionate; DSP; #22585, Thermo Fisher Scientific) treatment in 1 ml of DSP buffer (pH 7.4, 21 mM K_2HPO_4, 4 mM KH_2PO_4, and 200 mM sorbitol in ddH_2O) for 30 min at 30°C. The quenching reaction was performed with 50 mM Tris, pH 7.5, with incubation for 15 min at 30°C. Cell pellets were then suspended in 500 ml of lysis buffer (50 mM Tris pH 7.5, 50 mM NaCl, 10 mM $MgCl_2$, 1 mM EDTA, 5% glycerol, 0.1% Triton X-100, and a protease-inhibitor cocktail) and lysed with glass beads for 8 min at 4°C. The remaining cell pellets were collected and lysed again in 500 μl of lysis buffer. The cell lysates were clarified by centrifuging twice at 3500 × *g* for 5 min at 4°C. The clarified cell lysates were incubated with prewashed anti-HA magnetic beads (88836, Thermo Fisher Scientific) for 30 min at 4°C. The bound beads were washed with 1 ml of lysis buffer three times using a magnetic-particle concentrator (Dynal Biotech) and resuspended in 40 μl of sample buffer. Eluted protein complexes were boiled for 10 min at 95°C before SDS–PAGE analysis. Western blot analysis was conducted as described in our previous study (Wang *et al.*, 2022).

For the GST pull-down assay, *E. coli* strain BL21 (Novagen, La Jolla, CA) was transformed with pGEX-4T-1 plasmids expressing GST-tagged full-length Tlg1 or the cytosolic region of Tlg1 (amino acids 1–206). Bacterial cultures were grown in LB broth containing 0.1% ampicillin until an OD_{595} of 0.5 was achieved. Expression of recombinant proteins was induced by addition of 0.5 mM isopropyl β-D-1-thiogalactopyranoside for an additional 3 h at 37°C. Cells were harvested by centrifugation at 4°C and resuspended in ice-cold lysis buffer (1X PBS buffer pH 7.4, 1 mM DTT, 0.1% Triton X-100, and a protease-inhibitor cocktail). One mg/mL lysozyme was added to the lysis buffer and incubated on ice for 30 min. Cells were lysed by nitrogen decompression in a pressurized vessel (1500 psi) for 15 min at 4°C (Nitrogen Bomb, PARR 4639). The lysates were centrifuged at 10,000 × *g* for 10 min at 4°C. The supernatant was incubated with Glutathione Sepharose 4B (GE Healthcare, Amersham, Piscataway, NJ) for 2 h at 4°C. After 2 h of incubation, the bound beads were washed three times with 1 ml of lysis buffer and used for the GST pull-down assay. Yeast-cell lysates from *sft2*Δ cells coexpressing $Sft2^{FL}$-myc or $Sft2^{dN40}$-myc with HA-Snc1 were collected in lysis buffer (50 mM Tris pH 7.5, 50 mM NaCl, 10 mM $MgCl_2$, 1 mM EDTA, 5% glycerol, 0.1% Triton X-100, and a protease inhibitor cocktail) as described in the coimmunoprecipitation experiments. Ten μg of purified GST-tagged proteins were incubated in 1 ml of the collected yeast lysates for 1 h at 4°C. The bound beads were washed four times with 1 ml of lysis buffer and resuspended in 40 μl of sample buffer. The bound proteins were boiled at 95°C for 10 min before SDS-PAGE analysis. Western blot analysis was performed as described in our previous study (Wang *et al.*, 2022).

For coimmunoprecipitation assays in *sec18-1* cells, cells were transformed with HA-Snc1 or Sft2-myc. The following procedures were modified from previous studies (Holthuis *et al.*, 1998; Bryant and James, 2003). Seventy OD_{600} of early log-phase cells were harvested and washed with 1 ml of selection medium. Spheroplasts were generated as previously described (Wang *et al.*, 2022). Cells were treated with Zymolyase-100T (#120493, Ambio) and 1% β-mercaptoethanol in K-Pi buffer (190 mM K_2HPO_4, 310 mM KH_2PO_4, and 1.2 M sorbitol in ddH_2O) on an end-over-end rotator at 12 rpm at 24°C for 30 min. The spheroplasts were washed three times with 1 ml K-Pi buffer and then incubated with prewarmed medium containing 1 M sorbitol for 1 h at 24°C or 37°C. After 1 h of gentle shaking, the spheroplasts were washed with 1 ml K-Pi buffer and treated with 3 mM DSP in 1 ml of DSP buffer (pH 7.4, 21 mM K_2HPO_4, 4 mM KH_2PO_4, and 200 mM sorbitol in ddH_2O) for 30 min at 24°C. After quenching reaction, spheroplasts were lysed in lysis buffer containing glass beads as described in the co-IP experiments. An ATP-regenerating system (0.5 mM ATP, 40 mM creatine phosphate, and 0.1 mg/ml creatine kinase) was included in the lysis buffer. The clarified-cell lysates were incubated with prewashed anti-HA magnetic beads (88836, Thermo Fisher Scientific) for 2 h at 4°C. The bound beads were washed four times with 1 ml of lysis buffer using a magnetic-particle concentrator (Dynal Biotech) and resuspended in 40 μl of sample buffer. The eluted-protein complexes were boiled at 95°C for 10 min before SDS-PAGE analysis. Western-blot analysis was performed as described in our previous study (Wang *et al.*, 2022).

Yeast spotting assay for high-temperature sensitivity

Yeast strains expressing appropriate plasmids were cultured to mid-log phase in selection medium. Cells were then spotted onto synthetic medium plates at using 10-fold serial dilutions to observe growth. The plates were incubated at 30°C or 37°C for 3 d and imaged.

Quantification and statistical analysis

The quantification and statistical analyses were performed as previously described (Chen *et al.*, 2019; Wang *et al.*, 2022). For panels in all figures, *N* refers to the number of biological replicates and *n* refers to the sample size. In each experiment, at least 100 cells from three biological replicates were quantified. PM signals of GFP-Snc1 and cells containing GFP-Tlg1 or Vps53-mNeongreen (mNG) punctate signals were detected using ImageJ Fiji software.

For quantification in protein-interaction analyses, the association between Sft2 and its associated proteins was measured using ImageJ Fiji software. The intensities of target proteins were normalized to their respective input and HA-tagged proteins. For quantification in the GST pull-down assay, the intensities of $Sft2^{FL}$-myc, $Sft2^{dN40}$-myc, and HA-Snc1 were normalized to their respective input and the intensities of their respective GST-tagged proteins. For quantification of co-IP assays in *sec18-1* cells, the intensities of Tlg1 were normalized to their respective inputs and HA-Snc1 or Sft2-HA. Three independent experiments were analyzed using one-way ANOVA with Dunnett's post hoc multiple comparison test or unpaired *t* test. The binding intensity of the control in each experiment was used as the reference.

To quantify the colocalization of two proteins, the signals of GFP-Tlg1, GFP-Sft2, or GFP-Tlg2 overlapping with Sec7-mRFP were determined using the Manders' coefficient (Dunn *et al.*, 2011). Manders' coefficient was determined using ImageJ Fiji software with the Just Another Colocalization Plugin and Otsu automatic-image thresholding (Bolte and Cordelières, 2006; Dunn *et al.*, 2011; Pike *et al.*, 2017; Date *et al.*, 2022). Each yeast cell within the images was selected as a region of interest and the value of Manders' coefficient was determined according to Otsu automatic-image thresholding. The statistical analysis was performed by one-way ANOVA with Dunnett's post-hoc multiple-comparison test using the mean values of each biological replicate.

All statistical data in this study were analyzed using GraphPad Prism (GraphPad software) and presented as SuperPlots (Lord *et al*., 2020). The SuperPlots show individual data points from each biological replicate within an experiment in small circles with corresponding colors, the mean from each biological replicate in large circles, and the mean±SD of the means from each biological replicate. The same color of dots represents the data points in the same biological replicate. SuperPlots was used to account for the variability and reproducibility of each biological replicate. Statistical significance was determined using an unpaired *t* test or one-way ANOVA with Dunnett's post-hoc multiple-comparison tests. The control in each experiment was used as a reference for performing a one-way ANOVA with multiple comparisons. One-way ANOVA was used when multiple groups were compared, and the unpaired *t* test was used when two groups were compared. The corresponding statistics are listed in the respective figure legends. Significant differences (*$p < 0.05$; **$p < 0.005$; ***$p < 0.001$; ns, not significant) are indicated.

ACKNOWLEDGMENTS

We thank Drs. Randy Haun, Ya-Wen Liu, and Chia-Jung Yu for reviewing this manuscript. We thank Drs. Scott D. Emr, Todd R. Graham, Hugh R. Pelham, Chao-Wen Wang and Li-Ting Jang for providing us with the plasmids and yeast strains. We thank laboratory members Yi-Hsun Wang and Pei-Juan Cai for reagent preparation. We also thank the staff of the Biomedical Resource Center at the 1st Core Labs, National Taiwan University Medicine College, for technical assistance. This work was supported by grants from the Ministry of Science and Technology in Taiwan (MOST110-2320-B-002-068 and NSTC111-2634-F-002-017) and the Center of Precision Medicine by the Ministry of Education in Taiwan to F.S.L.

REFERENCES

Babazadeh R, Ahmadpour D, Jia S, Hao X, Widlund P, Schneider K, Eisele F, Edo LD, Smits GJ, Liu B, *et al*. (2019). Syntaxin 5 is required for the formation and clearance of protein inclusions during proteostatic stress. Cell Rep 28, 2096–2110.e2098.

Banfield DK, Lewis MJ, Pelham HR (1995). A SNARE-like protein required for traffic through the Golgi complex. Nature 375, 806–809.

Bean BD, Davey M, Conibear E (2017). Cargo selectivity of yeast sorting nexins. Traffic 18, 110–122.

Becker B, Schnöder T, Schmitt MJ (2016). Yeast reporter assay to identify cellular components of ricin toxin a chain trafficking. Toxins (Basel) 8, 366.

Behnia R, Panic B, Whyte JR, Munro S (2004). Targeting of the Arf-like GTPase Arl3p to the Golgi requires N-terminal acetylation and the membrane protein Sys1p. Nat Cell Biol 6, 405–413.

Benjamin JJ, Poon PP, Drysdale JD, Wang X, Singer RA, Johnston GC (2011). Dysregulated Arl1, a regulator of post-Golgi vesicle tethering, can inhibit endosomal transport and cell proliferation in yeast. Mol Biol Cell 22, 2337–2347.

Bolte S, Cordelières FP (2006). A guided tour into subcellular colocalization analysis in light microscopy. J Microsc 224(Pt 3), 213–232.

Bonifacino JS, Glick BS (2004). The mechanisms of vesicle budding and fusion. Cell 116, 153–166.

Bonifacino JS, Hierro A (2011). Transport according to GARP: receiving retrograde cargo at the trans-Golgi network. Trends Cell Biol 21, 159–167.

Bröcker C, Engelbrecht-Vandré S, Ungermann C (2010). Multisubunit tethering complexes and their role in membrane fusion. Curr Biol 20, R943–952.

Bryant NJ, James DE (2003). The Sec1p/Munc18 (SM) protein, Vps45p, cycles on and off membranes during vesicle transport. J Cell Biol 161, 691–696.

Chen KY, Tsai PC, Hsu JW, Hsu HC, Fang CY, Chang LC, Tsai YT, Yu CJ, Lee FJ (2010). Syt1p promotes activation of Arl1p at the late Golgi to recruit Imh1p. J Cell Sci 123(Pt 20), 3478–3489.

Chen KY, Tsai PC, Liu YW, Lee FJ (2012). Competition between the golgin Imh1p and the GAP Gcs1p stabilizes activated Arl1p at the late-Golgi. J Cell Sci 125(Pt 19), 4586–4596.

Chen YT, Wang IH, Wang YH, Chiu WY, Hu JH, Chen WH, Lee FS (2019). Action of Arl1 GTPase and golgin Imh1 in Ypt6-independent retrograde transport from endosomes to the trans-Golgi network. Mol Biol Cell 30, 1008–1019.

Christis C, Munro S (2012). The small G protein Arl1 directs the trans-Golgi-specific targeting of the Arf1 exchange factors BIG1 and BIG2. J Cell Biol 196, 327–335.

Conchon S, Cao X, Barlowe C, Pelham HR (1999). Got1p and Sft2p: membrane proteins involved in traffic to the Golgi complex. EMBO J 18, 3934–3946.

Date SS, Xu P, Hepowit NL, Diab NS, Best J, Xie B, Du J, Strieter ER, Jackson LP, MacGurn JA, *et al*. (2022). Ubiquitination drives COPI priming and Golgi SNARE localization. eLife 11, e80911.

Day KJ, Staehelin LA, Glick BS (2013). A three-stage model of Golgi structure and function. Histochem Cell Biol 140, 239–249.

Day KJ, Casler JC, Glick BS (2018). Budding yeast has a minimal endomembrane system. Dev Cell 44, 56–72.e54.

Diao A, Frost L, Morohashi Y, Lowe M (2008). Coordination of golgin tethering and SNARE assembly: GM130 binds syntaxin 5 in a p115-regulated manner. J Biol Chem 283, 6957–6967.

Dunn KW, Kamocka MM, McDonald JH (2011). A practical guide to evaluating colocalization in biological microscopy. Am J Physiol Cell Physiol 300, C723–742.

Ganley IG, Espinosa E, Pfeffer SR (2008). A syntaxin 10-SNARE complex distinguishes two distinct transport routes from endosomes to the trans-Golgi in human cells. J Cell Biol 180, 159–172.

Gurunathan S, Marash M, Weinberger A, Gerst JE (2002). t-SNARE phosphorylation regulates endocytosis in yeast. Mol Biol Cell 13, 1594–1607.

Hankins HM, Sere YY, Diab NS, Menon AK, Graham TR (2015). Phosphatidylserine translocation at the yeast trans-Golgi network regulates protein sorting into exocytic vesicles. Mol Biol Cell 26, 4674–4685.

Holthuis JC, Nichols BJ, Dhruvakumar S, Pelham HR (1998). Two syntaxin homologues in the TGN/endosomal system of yeast. EMBO J 17, 113–126.

Hong W, Lev S (2014). Tethering the assembly of SNARE complexes. Trends Cell Biol 24, 35–43.

Hsu JW, Tang PH, Wang IH, Liu CL, Chen WH, Tsai PC, Chen KY, Chen KJ, Yu CJ, Lee FJ (2016). Unfolded protein response regulates yeast small GTPase Arl1p activation at late Golgi via phosphorylation of Arf GEF Syt1p. Proc Natl Acad Sci USA 113, E1683–1690.

Ito H, Fukuda Y, Murata K, Kimura A (1983). Transformation of intact yeast cells treated with alkali cations. J Bacteriol 153, 163–168.

Lanz MC, Yugandhar K, Gupta S, Sanford EJ, Faça VM, Vega S, Joiner AMN, Fromme JC, Yu H, Smolka MB (2021). In-depth and 3-dimensional exploration of the budding yeast phosphoproteome. EMBO Rep 22, e51121.

Lewis MJ, Nichols BJ, Prescianotto-Baschong C, Riezman H, Pelham HR (2000). Specific retrieval of the exocytic SNARE Snc1p from early yeast endosomes. Mol Biol Cell 11, 23–38.

Liu YW, Huang CF, Huang KB, Lee FJ (2005). Role for Gcs1p in regulation of Arl1p at trans-Golgi compartments. Mol Biol Cell 16, 4024–4033.

Lord SJ, Velle KB, Mullins RD, Fritz-Laylin LK (2020). SuperPlots: communicating reproducibility and variability in cell biology. J Cell Biol 219, e202001064.

Lu L, Tai G, Hong W (2004). Autoantigen Golgin-97, an effector of Arl1 GTPase, participates in traffic from the endosome to the trans-golgi network. Mol Biol Cell 15, 4426–4443.

Mayer A, Wickner W, Haas A (1996). Sec18p (NSF)-driven release of Sec17p (alpha-SNAP) can precede docking and fusion of yeast vacuoles. Cell 85, 83–94.

McDonold CM, Fromme JC (2014). Four GTPases differentially regulate the Sec7 Arf-GEF to direct traffic at the trans-golgi network. Dev Cell 30, 759–767.

Munro S (2011). The golgin coiled-coil proteins of the Golgi apparatus. Cold Spring Harb Perspect Biol 3, a005256.

Papanikou E, Glick BS (2014). Golgi compartmentation and identity. Curr Opin Cell Biol 29, 74–81.

Paumet F, Brügger B, Parlati F, McNew JA, Söllner TH, Rothman JE (2001). A t-SNARE of the endocytic pathway must be activated for fusion. J Cell Biol 155, 961–968.

Pérez-Victoria FJ, Bonifacino JS (2009). Dual roles of the mammalian GARP complex in tethering and SNARE complex assembly at the trans-golgi network. Mol Cell Biol 29, 5251–5263.

Pike JA, Styles IB, Rappoport JZ, Heath JK (2017). Quantifying receptor trafficking and colocalization with confocal microscopy. Methods 115, 42–54.

Protopopov V, Govindan B, Novick P, Gerst JE (1993). Homologs of the synaptobrevin/VAMP family of synaptic vesicle proteins function on the late secretory pathway in *S. cerevisiae*. Cell 74, 855–861.
Reggiori F, Wang CW, Stromhaug PE, Shintani T, Klionsky DJ (2003). Vps51 is part of the yeast Vps fifty-three tethering complex essential for retrograde traffic from the early endosome and Cvt vesicle completion. J Biol Chem 278, 5009–5020.
Sambrook J, Russell DW (2001). Molecular Cloning: A Laboratory Manual. New York, NY: Cold Spring Harbor Laboratory Press.
Satpute-Krishnan P, Ajinkya M, Bhat S, Itakura E, Hegde RS, Lippincott-Schwartz J (2014). ER stress-induced clearance of misfolded GPI-anchored proteins via the secretory pathway. Cell 158, 522–533.
Schwabl S, Teis D (2022). Protein quality control at the Golgi. Curr Opin Cell Biol 75, 102074.
Setty SR, Shin ME, Yoshino A, Marks MS, Burd CG (2003). Golgi recruitment of GRIP domain proteins by Arf-like GTPase 1 is regulated by Arf-like GTPase 3. Curr Biol 13, 401–404.
Setty SR, Strochlic TI, Tong AH, Boone C, Burd CG (2004). Golgi targeting of ARF-like GTPase Arl3p requires its Nalpha-acetylation and the integral membrane protein Sys1p. Nat Cell Biol 6, 414–419.
Shin JJH, Crook OM, Borgeaud AC, Cattin-Ortolá J, Peak-Chew SY, Breckels LM, Gillingham AK, Chadwick J, Lilley KS, Munro S (2020). Spatial proteomics defines the content of trafficking vesicles captured by golgin tethers. Nature Communications 11, 5987.
Siniossoglou S, Pelham HRB (2001). An effector of Ypt6p binds the SNARE Tlg1p and mediates selective fusion of vesicles with late Golgi membranes. EMBO JJ 20, 5991–5998.
Song H, Orr AS, Lee M, Harner ME, Wickner WT (2020). HOPS recognizes each SNARE, assembling ternary trans-complexes for rapid fusion upon engagement with the 4th SNARE. eLife 9, e53559.
Sun Z, Brodsky JL (2019). Protein quality control in the secretory pathway. J Cell Biol 218, 3171–3187.
Tojima T, Suda Y, Ishii M, Kurokawa K, Nakano A (2019). Spatiotemporal dissection of the trans-Golgi network in budding yeast. J Cell Sci 132, jcs231159.
Torng T, Song H, Wickner W (2020). Asymmetric Rab activation of vacuolar HOPS to catalyze SNARE complex assembly. Mol Biol Cell 31, 1060–1068.
Travers KJ, Patil CK, Wodicka L, Lockhart DJ, Weissman JS, Walter P (2000). Functional and genomic analyses reveal an essential coordination between the unfolded protein response and ER-associated degradation. Cell 101, 249–258.
Tsai PC, Hsu JW, Liu YW, Chen KY, Lee FJ (2013). Arl1p regulates spatial membrane organization at the trans-Golgi network through interaction with Arf-GEF Gea2p and flippase Drs2p. Proc Natl Acad Sci USA 110, E668–677.
Tsvetanova NG (2013). The secretory pathway in control of endoplasmic reticulum homeostasis. Small GTPases 4, 28–33.
Tu Y, Zhao L, Billadeau DD, Jia D (2020). Endosome-to-TGN trafficking: organelle-vesicle and organelle-organelle interactions. Front Cell Dev Biol 8, 163.
Wang YH, Chiu WY, Chen YT, Cai PJ, Wu YC, Wu JL, Chen BH, Liu YW, Yu CJ, Lee FS (2022). Golgin Imh1 and GARP complex cooperate to restore the impaired SNARE recycling transport induced by ER stress. Cell Rep 38, 110488.
Whyte JR, Munro S (2002). Vesicle tethering complexes in membrane traffic. J Cell Sci 115, 2627–2637.
Witkos TM, Lowe M (2015). The golgin family of coiled-coil tethering proteins. Front Cell Dev Biol 3, 86.
Wong M, Gillingham AK, Munro S (2017). The golgin coiled-coil proteins capture different types of transport carriers via distinct N-terminal motifs. BMC Biology 15, 3.
Xu P, Hankins HM, MacDonald C, Erlinger SJ, Frazier MN, Diab NS, Piper RC, Jackson LP, MacGurn JA, Graham TR (2017). COPI mediates recycling of an exocytic SNARE by recognition of a ubiquitin sorting signal. eLife 6, e28342.
Yoon TY, Munson M (2018). SNARE complex assembly and disassembly. Curr Biol 28, R397–R401.
Yu CJ, Lee FJ (2017). Multiple activities of Arl1 GTPase in the trans-Golgi network. J Cell Sci 130, 1691–1699.
Zhou T, Lu Y, Xu C, Wang R, Zhang L, Lu P (2020). Occludin protects secretory cells from ER stress by facilitating SNARE-dependent apical protein exocytosis. Proc Natl Acad Sci USA 117, 4758–4769.
Zhou X, Li W, Liu Y, Amon A (2021). Cross-compartment signal propagation in the mitotic exit network. eLife 10, e63645.
Zielinska DF, Gnad F, Schropp K, Wiśniewski JR, Mann M (2012). Mapping N-glycosylation sites across seven evolutionarily distant species reveals a divergent substrate proteome despite a common core machinery. Mol Cell 46, 542–548.